

Sol–gel derived Si/C/O/N-materials: molecular model compounds, xerogels and porous ceramics[†]

Hui-Jie Cheng^{a,b}, Katrin Lippe^b, Edwin Kroke^{b*}, Jörg Wagler^b, Gerrit W. Fester^b, Ya-Li Li^a, Marcus R. Schwarz^b, Tatyana Saplinova^b, Stefanie Herkenhoff^c, Vladislav Ischenko^c and Jörg Woltersdorf^c



Polymeric Si/C/O/N xerogels, with the idealized polymer network structure comprising $[\text{Si}-\text{O}-\text{Si}(\text{N}=\text{C}=\text{N})_3]_n$ moieties, were prepared by reactions of hexachlorodisiloxane ($\text{Cl}_3\text{Si}-\text{O}-\text{SiCl}_3$) with *bis*(trimethylsilyl)carbodiimide ($\text{Me}_3\text{Si}-\text{N}=\text{C}=\text{N}-\text{SiMe}_3$, BTSC). NMR and FTIR spectra indicate the existence of $-\text{N}=\text{C}=\text{N}-$ and $-\text{Si}-\text{O}-\text{Si}-$ units in the xerogels and also in the ceramic materials obtained upon pyrolysis. The feasibility of this reaction protocol was confirmed on the molecular level by the deliberate synthesis of the macrocyclic compound $[\text{SiPh}_2-\text{O}-\text{SiPh}_2(\text{N}=\text{C}=\text{N})_2]_2$, the crystal structure and spectroscopic data of which are reported. The influence of pyridine as a catalyst for the cross-linking reaction was studied. The degree of cross-linking increased within the polymers with the addition of pyridine. It was shown by the reaction of hexachlorodisiloxane with excess pyridine that the latter appears to activate only one out of the two $-\text{SiCl}_3$ moieties under formation of hexacoordinated silicon compounds. The crystal structure of $\text{Cl}_3\text{Si}-\text{O}-\text{SiCl}_3(\text{pyridine})_2$ is presented. Quantum chemical calculations are in support of this adduct being a potential intermediate in the pyridine catalyzed sol–gel process. The ceramic yield after pyrolysis of the Si/C/O/N-xerogels at 1000°C , which reaches values up to 50%, was found to depend on the aging protocol (time, temperature), whereas no correlation was found with the amount of pyridine added for xerogel synthesis. The Si/C/N/O-ceramics obtained after pyrolysis at 1000°C under NH_3 are completely amorphous. Chemically they have to be considered as hybrids between an ideal $[\text{SiOSi}(\text{NCN})_3]_n$ network and glass-like $\text{Si}_2\text{N}_2\text{O}$. The products are mesoporous with closed pores and a broad pore size distribution. Copyright © 2011 John Wiley & Sons, Ltd.

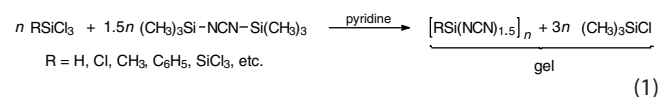
Supporting information may be found in the online version of this article.

Keywords: Si/C/O/N; sol–gel process; silicon carbodiimide; hexachlorodisiloxane; nonhydrolytic; quantum mechanical calculations

Introduction

The sol–gel route to inorganic materials and ceramics has the advantages of flexible processing, product homogeneity, diversity of accessible elemental compositions, as well as much lower processing temperatures compared with conventional techniques.^[1–3] In the past decades, this synthesis method has been investigated in detail and developed to prepare various porous as well as nonporous materials. Most of the research in this field has dealt with hydrolytic sol–gel routes to oxides. Numerous reports have been published on the incorporation of hetero-elements E such as boron^[4] or aluminum^[5] into the gels in order to modify and improve the properties of the final Si/E/C/O-ceramics.

Since the discovery of gel-forming reactions of tetrachlorosilane SiCl_4 ,^[6,7] methyltrichlorosilane MeSiCl_3 ^[8,9] and other trichlorosilanes RSiCl_3 (with R = H, alkyl, aryl)^[10,11] as well as selected dichlorosilanes^[12–14] with *bis*(trimethylsilyl)carbodiimide (BTSC), this novel anhydrous technique has been further investigated and applied to produce organic–inorganic hybrid materials^[15] and various nonoxide ceramics [eqn (1)].



Although such sol–gel processes are nonoxidic and nonhydrolytic, there is a characteristic analogy to the oxide systems. Owing to the pseudo-chalcogenic character of the carbodiimide group, it adopts the role of the oxygen atom, whereas the trimethylsilyl group can be considered as an analog of the protons in a hydrolytic process.^[13,16,17] Several materials in the systems Si/C,^[18] B/C/N,^[19,20] Si/C/N,^[21,22] Si/B/C/N,^[23–25] and Si/Al/C/N^[26] possessing high thermal resistance and chemical stability, have been synthesized using this particular kind of sol–gel route. Several further reports on related work on BTSC-derived element carbodiimides and their use as precursors for hybrid and ceramic

* Correspondence to: Edwin Kroke, Institut für Anorganische Chemie, TU Bergakademie Freiberg, Freiberg 09596, Germany.
E-mail: Edwin.Kroke@chemie.tu-freiberg.de

a Key laboratory of Advanced Ceramics and Machining Technology, Tianjin University, Ministry of Education, Tianjin 300072, China

b Institut für Anorganische Chemie, TU Bergakademie Freiberg, Freiberg D-09596, Germany

c Max-Planck-Institut für Mikrostrukturphysik, Weinberg 2, D-06120 Halle, Germany

† In memoriam Professor Jörg Woltersdorf.

materials have been published. Among these studies are gallium carbodiimides^[27] and several transition metal compounds.^[28] Recent studies on polysilylcarbodiimides were devoted to their enthalpy of formation^[29] and use as stabilizers.^[30]

Neither the controlled incorporation of oxygen into silylcarbodiimide gels, nor the controlled incorporation of carbodiimide groups into conventionally-produced polysiloxanes, leading to the hybrid polysiloxane/polysilylcarbodiimide gels and related Si/C/O/N ceramic materials, has been reported so far. In particular, Si/C/O/N ceramics derived from the above-mentioned hybrid gels might be technologically interesting, combining enhanced oxidation resistance compared with Si/(C)/N materials, and improving thermo mechanical properties compared with Si/(C)/O glasses and ceramics.

In the present work, the hybrid polysiloxane/polysilylcarbodiimide gels were synthesized by the reaction between BTSC and hexachlorodisiloxane, with the aim to produce suitable precursors for the preparation of Si/C/O/N ceramics upon their subsequent pyrolysis. The effect of pyridine as a catalyst on the cross-linking degree of the Si/C/O/N-polymers as well as on the composition, structure and morphology of the derived ceramics has been studied along with the aging temperature and the aging time.

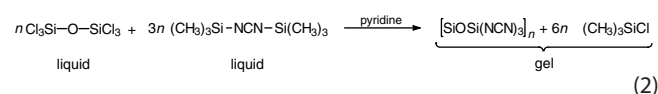
Experimental

General Considerations

Owing to the air and moisture sensitivity of silylcarbodiimides, all reactions were performed in heat-gun dried glass vessels in a glovebox (N₂ atmosphere, O₂ < 0.1 ppm, H₂O < 0.1 ppm) or in an argon flow, using the Schlenk technique.^[31] Hexachlorodisiloxane (Sigma-Aldrich Chemie GmbH, 96%) and 1,3-dichloro-1,1,3,3-tetraphenyldisiloxane (ABCR) were used without further purification. *Bis*(trimethylsilyl)carbodiimide was prepared from hexamethyldisilazane (Me₃Si-NH-SiMe₃, Sigma-Aldrich Chemie GmbH, 99%) and cyanoguanidine [HN=C(NH₂)NHCN, Sigma-Aldrich Chemie GmbH, 99%] according to the literature.^[32] Dried cyclohexane (Sigma-Aldrich Chemie GmbH, 99.5%) was stored in a glovebox and used directly as a solvent without further purification. Tetrahydrofuran (THF), toluene and triethylamine were distilled from sodium/benzophenone ketyl and stored under argon atmosphere.

Preparation of Si/C/O/N Gels

Synthesis of the gels proceeds according to the following idealized reaction [eqn (2)]:



A homogeneous mixture of 1.20 ml (4.46 mmol) of hexachlorodisiloxane and 4.10 ml (18.06 mmol) of BTSC was prepared in a Schlenk tube prior to addition of pyridine (Py). The different amounts of Py [molar ratios of Py/BTSC = 0, 0.05, 0.10, 0.15, 0.20; with cyclohexane (1.2 ml) as solvent, or without any solvent] were dropped into the mixture of starting materials while shaking the Schlenk tube at the same time. Upon addition of small amounts of pyridine traces of solid pyridine hydrochloride precipitated, owing to very small amounts of HCl present in the chlorosiloxane.

This solid sticks to the walls of the Schlenk tubes, and can therefore easily be removed before gelation by transferring the reaction solution to another flask. In the samples with larger fractions of pyridine added, the formation of notable amounts of solid precipitates was observed, resulting from the formation of adducts of hexachlorodisiloxane with pyridine (see below). The reaction mixtures were then incubated at 45, 75 or 90 °C (without stirring) until gelation occurred. Gelation points were visually determined simply by turning the flask over. The gelation time depends on the temperature applied and the amount of the catalyst used. For further cross-linking, different aging times (ranging between 7 and 30 days) were applied. The liquid components of the gels (i.e. the by-product chlorotrimethylsilane, the solvent cyclohexane, as well as residual BTSC and pyridine) were removed in vacuum followed by drying at 160 °C/10⁻² mbar/4 h to obtain the xerogels.

Synthesis of Si/C/O/N Ceramics

The xerogels were transferred to quartz boats and pyrolyzed in a stream of dry ammonia in a quartz Schlenk tube. Applied heating rates were 5 °C min⁻¹. The time of exposure at 1000 °C was 2 h in all cases.

Synthesis and Characterization of cyclo-[Ph₂Si-O-SiPh₂(NCN)]₂

A solution of 1,3-dichloro-1,1,3,3-tetraphenyldisiloxane (5.37 g, 11.9 mmol) and triethylamine (2.41 g, 23.8 mmol) in THF (70 ml) was stirred at 0 °C and a solution of cyanamide (0.50 g, 11.9 mmol) in THF (8 ml) was added dropwise (causing the immediate precipitation of triethylamine hydrochloride). Upon complete addition of the cyanamide solution the mixture was heated and kept under reflux conditions for 1.5 h and then stored at room temperature overnight. The triethylamine hydrochloride was then filtered off and washed with THF (20 ml). From the combined filtrate and washings the solvent was removed under reduced pressure, and the solid (but somewhat oily) residue was recrystallized from a mixture of hexane (5 ml) and THF (10 ml). After some crystalline product had formed additional hexane (5 ml) was layered over the product solution before it was then stored at 6 °C for one week. The crystalline colorless product was filtered off, washed with hexane (3 ml) and dried in a vacuum (2.34 g). From the combined filtrate and washings some solvent (ca. 5 ml) was removed under reduced pressure and the solution was again stored at 6 °C to give a second fraction of the product (0.72 g). A third fraction of the product was isolated after cooling the solution to -25 °C (0.30 g). Yield: 3.36 g (3.99 mmol, 67%). M.p. 197–199 °C (in sealed capillaries). ¹H NMR (400.1 MHz, CDCl₃) δ = 7.27 (m, 16 H, *meta*), 7.39 (t, 8 H, 7.4 Hz, *para*), 7.57 (d, 16 H, 7.4 Hz, *ortho*). ¹³C NMR (100.6 MHz, CDCl₃) δ = 122.0 (N=C=N), 127.9 (*ortho*), 130.4 (*ipso*), 133.7 (*para*), 134.2 (*meta*). ²⁹Si NMR (79.5 MHz, CDCl₃) δ = -42.9. Elemental analysis calcd for C₅₀H₄₀N₄O₂Si₄ (841.2 g mol⁻¹): C, 71.4; H, 4.79; N, 6.66. Found: C, 70.9; H, 4.91; N, 6.77. X-ray structure analysis (CCDC 781 896): crystal dimensions 0.50 × 0.38 × 0.18 mm, C₅₀H₄₀N₄O₂Si₄, M_r = 841.22, T = 180(2) K, triclinic, space group P $\bar{1}$, a = 9.2415(7), b = 10.6542(7), c = 12.4571(9) Å, α = 75.691(2), β = 73.965(2), γ = 78.193(2)°, V = 1129.94(14) Å³, Z = 1, ρ_{calcd} = 1.236 Mg m⁻³, μ(Mo-Kα) = 0.176 mm⁻¹, F(000) = 440, 2θ_{max} = 54.0°, 20014 collected reflections, 4803 unique reflections (R_{int} = 0.0271), 307 parameters, S = 1.076, R₁ = 0.0372 [I > 2σ(I)], wR₂ (all data) = 0.1076, maximum/minimum residual electron density +0.360/-0.239 e Å⁻³.

Synthesis and Characterization of $\text{Cl}_3\text{Si-O-SiCl}_3(\text{Pyridine})_2$

To a cooled solution (dry *iso*-propanol, -78°C) of hexachlorodisiloxane (1.43 g, 5.00 mmol) in toluene (20 ml) was added pyridine (1.58 g, 20.0 mmol), whereupon a white precipitate formed. The mixture was stirred at -78°C for 1 h and then allowed to adapt to room temperature. The white solid product was then filtered off, washed with toluene and dried in a vacuum. Yield: 1.55 g (3.50 mmol, 70%). This compound exhibits poor solubility in nonpolar solvents such as toluene or hexane, whereas it dissociates into hexachlorodisiloxane and pyridine in chloroform. Hence, characterization was limited to the solid state. ^{13}C CP/MAS NMR: $\delta = 124.7, 130.1, 145.1$; ^{29}Si CP/MAS NMR: $\delta = -53.5$ (OSiCl_3), -180.5 ($\text{OSiCl}_3\text{Py}_2$). Elemental analysis calcd for $\text{C}_{10}\text{H}_{10}\text{Cl}_6\text{N}_2\text{OSi}_2$ (443.1 g mol $^{-1}$): C, 27.8; H, 2.31; N, 6.52. Found: C, 27.8; H, 2.33; N, 6.48. X-ray structure analysis (CCDC 781 895): crystal dimensions $0.38 \times 0.20 \times 0.02$ mm, $\text{C}_{10}\text{H}_{10}\text{Cl}_6\text{N}_2\text{OSi}_2$, $M_r = 443.08$, $T = 100(2)$ K, monoclinic, space group $P2_1/c$, $a = 13.0395(14)$, $b = 6.9499(8)$, $c = 19.675(2)$ Å, $\beta = 95.897(3)^\circ$, $V = 1773.6(3)$ Å 3 , $Z = 4$, $\rho_{\text{calcd}} = 1.659$ Mg m $^{-3}$, $\mu(\text{Mo-K}\alpha) = 1.101$ mm $^{-1}$, $F(000) = 888$, $2\theta_{\text{max}} = 50.0^\circ$, 9094 collected reflections, 3128 unique reflections ($R_{\text{int}} = 0.0563$), 204 parameters, $S = 1.034$, $R_1 = 0.0496$ [$I > 2\sigma(I)$], $wR_2(\text{all data}) = 0.1087$, maximum/minimum residual electron density $+0.523/-0.379$ e Å $^{-3}$. The data set was collected from a slightly twinned crystal. De-twinning was performed after initial structure solution and refinement using TwinRotMat as implemented in WinGX Platon and a HKLF5-file was written for the final stages of the refinement, which revealed twin populations of 96 and 4%. The twin law found, ca. (1 0 0)(0 -1 0)(-0.333 0 -1), corresponds to a 180° rotation about axis [1 0 0].

Si/C/O/N Xerogel and Ceramics Characterization

The carbon content of the products was determined by combustion analysis (LECO RC-412 carbon analyzer). Oxygen and nitrogen contents were measured by hot gas extraction at 2500°C in helium atmosphere (LECO TC-436). Additionally, C/H/N-combustion analyses were performed using a CHN analyzer (Micro Cube, Elementar, Hanau). For the determination of the chlorine content the xerogels were dissolved in aqueous NaOH solution at pH 11, then analyzed by ion chromatography, using a standard NaCl solution as reference.

The chemical structures of the products were investigated by FT-IR spectroscopy (Varian Excalibur 3100 with 4 cm $^{-1}$ resolution) using the KBr method, Raman spectroscopy (Bruker RFS 100/s with capillary glass, laser wavelength 1064 nm) and cross-polarization/magic-angle-spinning nuclear magnetic resonance spectroscopy (CP/MAS NMR Bruker Avance TM WB 400 MHz spectrometer with a ^{29}Si resonance frequency of 79.51 MHz, spinning rate 5 kHz). Inside a glove box the xerogels were compressed in small Kelf inserts prior to placing them in 7 mm zirconia spinners for ^{29}Si and ^{13}C CP/MAS NMR measurements.

Scanning electron microscopy (SEM, LEO 1530 FEG, Carl Zeiss NTS GmbH, Oberkochen, Germany, with acceleration voltage of 12 kV, and Tescan VEGA II SBH, 20 kV) was used to characterize the microstructure of the xerogels. The samples were handled under an inert atmosphere to avoid hydrolysis. For EDX analysis during the SEM studies a Bruker AXS X-Flash4010 with silicon drift detector and a 8 μm ultrathin polymer-coated Be window (for light elements) was used together with Quantax 400 software for spectrum recording and data processing.

Nitrogen adsorption isotherms of xerogels were determined by an AREA meter (Ströhlein GmbH und Co. Pressure 0.5–1.0 mbar,

N_2 , at $30-300^\circ\text{C}$), and analyzed using the BET (Brunauer-Emmett-Teller) model. The pyrolysis of the xerogels was studied by thermal analysis under an argon flow (TG/DTA 22, Seiko Instrument, heating rate 5°C min^{-1} , maximum temperature 1000°C).

The morphology of the mesopores in the pyrolyzed samples was investigated by high resolution transmission electron microscopy (HR-TEM) using a CM 20 FEG electron microscope (Philips, Eindhoven, Netherlands; operating voltage of 200 kV), equipped with a post-column electron energy filter (Gatan Imaging Filter GIF 200, model 667, Pleasanton, CA).

Theoretical Methods

Geometry optimization and single point energy calculation have been performed with GAMESS-US^[33] program in the framework of the density functional theory (DFT). In case of the isodesmic reaction, geometry optimization and zero-point energy calculations were carried out with a 6-31G* basis set along with the B3LYP hybrid exchange correlation functional. For single point energy calculations the B3LYP functional was used with a TZV + (2df,1p) basis set.

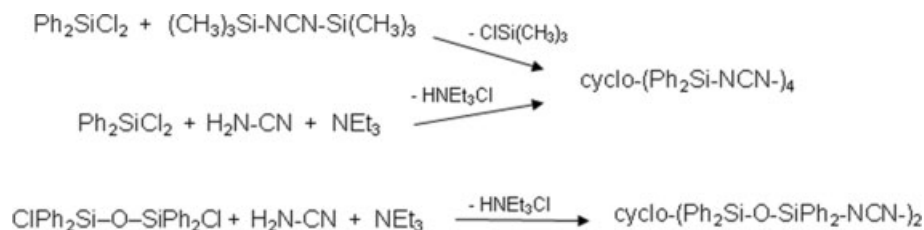
The B3LYP hybrid exchange-correlation functional was used along with a 6-31G* Gaussian-type basis set for the geometry optimization of the pyridine-adduct complexes. Thereby, in a first run the Si-N bond length was fixed at 1.8 Å, whereas the other parts of the molecule were fully optimized. In successive cycles the restraint on the Si-N bond was lifted as well. prior to full optimization of all parameters including the Si-N bond. Single-point energy calculations have been performed with a 6-311G + (2d,p) basis set along with the B3LYP hybrid exchange correlation functional. The natural charges were obtained from calculations with NBO 5.0.^[34]

Results and Discussion

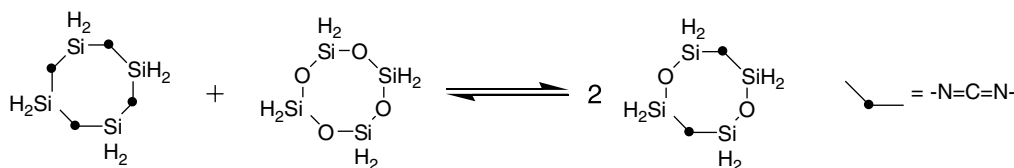
Synthesis of a Molecular Model Compound for Siloxane/silylcarbodiimide Containing Oligomers and Polymers

In a previous report we have shown that from diphenyldichlorosilane oligomeric (cyclic) silylcarbodiimides can be prepared via different routes, i.e. via condensation with BTSC and via base-supported HCl-elimination with cyanamide.^[13] (Scheme 1, top). The latter route proved also feasible to create mixed siloxane/silylcarbodiimide-functionalized heterocycles with alternating Si-O-Si and Si-N=C=N-Si sequences, the use of chlorosiloxanes being a prerequisite (Scheme 1, bottom). This synthesis route delivered the macrocyclic compound cyclo-[Ph $_2$ Si-O-SiPh $_2$ (NCN)] $_2$ in good yield (67% isolated). A 12-membered cycle consisting of a [Si-O-Si-(NCN)] $_2$ sequence could thus be also a favorable structural motive in the formation of carbodiimide gels from 1,3-(oligo)chloro-functionalized disiloxanes.

The ^{29}Si NMR spectrum of cyclo-[Ph $_2$ Si-O-SiPh $_2$ (NCN)] $_2$ ($\delta = -42.9$ ppm in CDCl_3) is very similar to that of octaphenylcyclotetrasiloxane ($\delta = -43.0$ ppm in dioxane) and the fully carbodiimide bridged system [Ph $_2$ Si(NCN)] $_4$ ($\delta = -44.4$ ppm in dioxane)^[13]. Considering a [Si-O-Si(NCN)] $_2$ 12-membered cyclus in an isodesmic reaction;^[35] this reaction can be written like in Scheme 2, where the tetramer carbodiimide and the cyclotetrasiloxane act as counterparts. Such an isodesmic reaction can be used to quantify the stability of mixed siloxane/silylcarbodiimides by calculating the reaction enthalpy of this hypothetical reaction according to eqn (3). The reaction enthalpy for the reaction in



Scheme 1. Synthesis of phenyl-substituted cyclo-tetrasilylcarbodiimide using *bis*(trimethylsilyl)carbodiimide (BTSC) or cyanamide/triethylamine as starting materials (top) and the first ‘mixed’ siloxane/silylcarbodiimide using the educt 1,3-dichloro-1,1,3,3-tetraphenyldisiloxane (bottom).



Scheme 2. Hypothetic isodesmic reaction to form cyclo-[H₂Si-O-SiH₂(NCN)]₂ starting from cyclo-tetrasilylcarbodiimide and cyclo-tetrasiloxane.

Scheme 2 has been calculated as 0.91 kcal mol⁻¹, and therefore the reaction should be endothermic in the gas phase. This enthalpy is quite small and may be reverted to exothermic value by solvent effects, thus supporting a certain relevance of mixed siloxane/silylcarbodiimide macrocyclic systems also in the case of partially hydrolyzed silylcarbodiimide gels.

$$\begin{aligned}
 H_{\text{rct.}} &= 2 \Delta H_f^\circ [(\text{H}_2\text{Si})_4\text{O}_2(\text{NCN})_2] \\
 &- \{ \Delta H_f^\circ [(\text{H}_2\text{Si})_4(\text{NCN})_4] + \Delta H_f^\circ [(\text{H}_2\text{Si})_4\text{O}_4] \} \quad (3)
 \end{aligned}$$

The molecular structure of cyclo-[Ph₂Si-O-SiPh₂(NCN)]₂ was determined by single crystal X-ray diffraction analysis (Fig. 1). The discussion of the bonding properties of the carbodiimide moiety is limited by a twofold disorder (cross-wise about C1). Despite this effect, the structure reveals an almost planar arrangement of this 12-membered heterocycle. The bonding parameters (Si-O and Si-N bond lengths) are in the expected range for siloxanes and silylcarbodiimides, respectively, and the wide Si-O-Si and Si-N-C angles reflect similar behaviour as in octaphenyldisiloxane and [Ph₂Si(NCN)]₄.

Formation of Siloxane/silylcarbodiimide Xerogels – Cl₃Si-O-SiCl₃(py)₂ as an Intermediate

The hybrid polysiloxane/polysilylcarbodiimide gels were synthesized by reactions between BTSC and hexachlorodisiloxane. BTSC was used in excess, since it was observed in former studies that this leads to lower chlorine contents of the gels and xerogels in many cases. Table 1 summarizes the experimental conditions. The time to the gelation point depends strongly on the amount of the catalyst (pyridine) used and on the reaction temperature (see below). Nevertheless, given sufficient reaction time, gels were obtained for all reaction batches without exception.

Mixtures without pyridine remain liquid for several hours and then turn into homogeneous gels. However, from the first drop of pyridine added at room temperature, the mixtures react violently, especially if no solvent is present. This exothermic reaction can be attributed to the formation of chlorosilane-pyridine adducts of the type [RSiCl₃·2Py] (R = H, alkyl, aryl, Cl, etc.). These adducts containing hexa-coordinated silicon atoms tend to precipitate owing to their low solubility in many organic solvents.^[36]

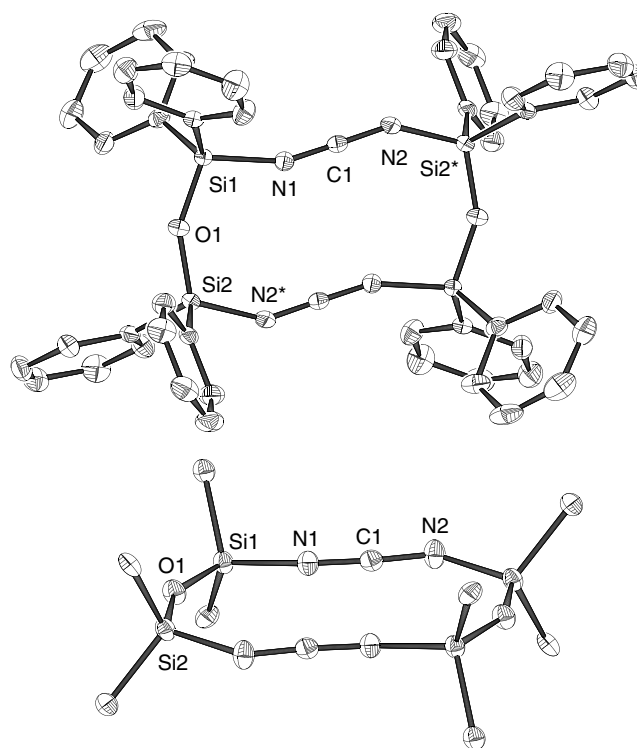


Figure 1. ORTEP diagram (thermal ellipsoids with 30% probability) of cyclo-[Ph₂Si-O-SiPh₂-(NCN)]₂ in the crystal. The asymmetric unit consists of a half-molecule, which is located around a center of inversion. Selected atoms are labeled; asterisked labels represent symmetry equivalents. The carbodiimide group is two-fold disordered (site occupancy 0.5 each position); only one orientation is depicted. Selected bond lengths (pm) and angles (deg): Si1-O1 162.3(1), Si2-O1 162.7(1), Si1-N1 171.7(2), Si2-N2* 171.6(2), N1-C1 120.5(2), N2-C1 120.5(2), Si1-O1-Si2 151.1(1), Si1-N1-C1 157.9(5), Si2*-N2-C1 145.4(5), N1-C1-N2 176.5(5).

Formation of related adducts of chorosilanes has already been studied.^[37–40] In case of hexachlorodisiloxane, however, questions arise concerning the composition of the adduct (pyridine attached to one or two of the silicon atoms) as well as its relevance in a system containing an excess hexachlorodisiloxane but under-stoichiometric amounts of pyridine. The first question

Table 1. Experimental conditions of the formation of Si/C/O/N gels from hexachlorodisiloxane (O) and *bis*(trimethylsilyl)carbodiimide (BTSC) with or without cyclohexane as solvent and pyridine (Py) as catalyst. The syntheses were conducted at different temperatures (45, 75 and 90 °C) in nitrogen atmosphere. As an example, the table shows the data for 75 °C

Sample no.	O/BTSC/Py ^a (molar ratio)	The time to gelation point (h)	Aging time (days)
1	1 : 3 : 0	18	7 and 30
2	1 : 3 : 0.15	9	7 and 30
3	1 : 3 : 0.3	5	7 and 30
4	1 : 3 : 0.45	4	7 and 30
5	1 : 3 : 0.6	2	7 and 30

^aSince pyridine reacts with chlorosilane to form adducts which precipitate, the concentration of pyridine in solution is lower than the provided values.

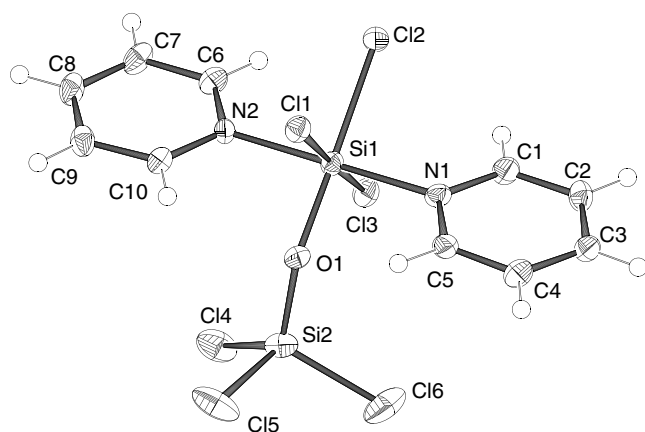


Figure 2. ORTEP diagram (thermal ellipsoids with 50% probability) of $\text{Cl}_3\text{Si}-\text{O}-\text{SiCl}_3(\text{Py})_2$ in the crystal. The trichlorosilyl group is two-fold disordered (site occupancies 0.86 and 0.14); only the predominant part is depicted. Selected bond lengths (pm) and angles (deg): Si1-Cl1 222.8(2), Si1-Cl2 221.6(2), Si1-Cl3 218.9(2), Si1-N1 195.4(4), Si1-N2 197.0(4), Si1-O1 170.0(3), Si2-O1 158.0(3), Si2-Cl4 202.8(2), Si2-Cl5 202.3(2), Si2-Cl6 202.0(2), Si1-O1-Si2 149.0(2), O1-Si1-Cl2 177.6(2), Cl1-Si1-Cl3 178.1(1), N1-Si1-N2 179.0(2).

could be answered by deliberate synthesis of the complex $\text{Cl}_3\text{Si}-\text{O}-\text{SiCl}_3(\text{pyridine})_2$. Although excess pyridine was utilized in this synthesis, only one of the two silicon atoms is hexacoordinate, whereas tetracoordination of the other $\text{O}-\text{SiCl}_3$ -group is retained. This was confirmed by both X-ray diffraction analysis (Fig. 2) and by ^{29}Si CP/MAS NMR analysis for the gross product. The latter clearly shows a peak characteristic of tetracoordinate OSiCl_3 groups (at -53.5 ppm, slightly upfield with respect to hexachlorodisiloxane, which has a signal at -45.45 ppm^[41]) and a significantly upfield-shifted resonance at -180.5 ppm for the hexacoordinate silicon atoms. The upfield shift of the tetracoordinate Si atom's NMR signal may be interpreted as a result of Si-O bond strengthening. Whereas the Si-O bond to the hexacoordinate Si atom is rather long [170.0(3) pm], this bond lengthening upon pyridine coordination gives rise to a shortening of the second Si-O bond [to 158.0(3) pm], whereas for hexachlorodisiloxane a slightly longer Si-O bond length of 159.2 ± 1.0 pm was reported (results of gas phase electron diffraction analysis).^[42] The Si-O-Si angle [149.0(2)°] is similar to that of hexachlorodisiloxane (in the gas

phase), which was determined to be $146 \pm 4^\circ$. This Si-O-Si bond angle in $\text{Cl}_3\text{Si}-\text{O}-\text{SiCl}_3(\text{Py})_2$ allows for Cl-capping of one of the tetrahedral faces of Si2 by Cl3 from a distance of 343.6(2) pm, which might also contribute to the upfield shift of the ^{29}Si NMR signal. With respect to Si-Cl bond activation by pyridine coordination, one can discern a notable Si-Cl bond lengthening upon hexacoordination (from ca. 202 to ca. 220 pm). The differences between the longer bonds Si1-Cl1, Si1-Cl2 (223 and 222 pm, respectively) and the somewhat shorter bond Si1-Cl3 (219 pm) is mainly based on packing effects. Whereas the former establish 5 $\text{Cl}\cdots\text{H}$ contacts each within a distance of ca. 320 pm, the environment of the latter exhibits only four of them.

The stability of pyridine adducts and in turn their relevance as intermediates in the pyridine catalyzed sol-gel-process was also investigated by computational methods. For the monodentate ligand pyridine there are four different types of 1:1 complexes (**Ia-d**, Fig. 3) theoretically possible. In the case of the 1:2 complexes there are three isomers with only one silicon atom coordinated by two pyridine molecules (**Ila-c**, Fig. 3) as well as 10 additional different complexes if the pyridine molecules are coordinated at both silicon atoms. Out of these complexes only the one shown in Fig. 3 (**IId**) has been calculated. For complexes with a 1:4 silane:pyridine ratio complex **IV** in Fig. 3 out of all six theoretically possible complexes was considered.

Optimization converged to the geometries depicted in Fig. 4 and selected parameters thereof are presented in Table 2. Whereas the pentacoordinate silicon complex with pyridine and the $-\text{OSiCl}_3$ moiety in axial positions (**Ia**) proved less stable and converged to molecular structures with a long (>3 Å) Si-N bond, those with an angle smaller than 180° between pyridine and $-\text{OSiCl}_3$ turned out to have positive relative energies with respect to hexachlorodisiloxane and pyridine. At the hexacoordinated silicon atoms (**Ila-c**) and the pentacoordinated Si atoms in **IId** the respective configuration was retained during optimization, and the structure **Ila** with *trans* disposed N atoms proved to be the most stable. According to these data in a reaction from hexachlorodisiloxane and pyridine the complex **Ila** should be formed, which is confirmed by the above results of the X-ray diffraction analysis of $\text{Cl}_3\text{Si}-\text{O}-\text{SiCl}_3(\text{pyridine})_2$.

Finally, optimization of **IV** confirmed that the addition of four pyridine molecules under formation of a disiloxane with two hexacoordinate Si atoms should be less favorable, thus being in accordance with the isolation of the adduct $\text{Cl}_3\text{Si}-\text{O}-\text{SiCl}_3(\text{pyridine})_2$.

Characterization of Siloxane/Silylcarbodiimide Xerogels Obtained from Hexachlorodisiloxane and BTSC

Si/C/O/N gels and xerogels were synthesized by a standard procedure. Details concerning synthesis parameters including temperature, aging time, drying conditions are summarized in the Experimental section. The elemental analysis data of a typical xerogel obtained from hexachlorodisiloxane is as follows: C, 15–20; N, 25–30; O, 8.0–8.5; H, 1.0–1.8; Cl, 1.0–3.0 (weight-%). The ideal composition of the silyloxycarbodiimide $[\text{SiOs}(\text{NCN})_3]_n$ is: C, 18.8; N, 43.8; O, 8.3. The deviation from the ideal formula can (at least in part) be attributed to remaining $-\text{N}=\text{C}=\text{N}-\text{SiMe}_3$ substituents.^[43,44] Incomplete substitution and condensation reactions cause both the residual chlorine content and hydrogen content.

^{29}Si NMR spectra for samples *without pyridine* as a catalyst (Fig. 5a) revealed several distinct signals: The broad resonance with high intensity at ca. -103 ppm is assigned to silicon atoms

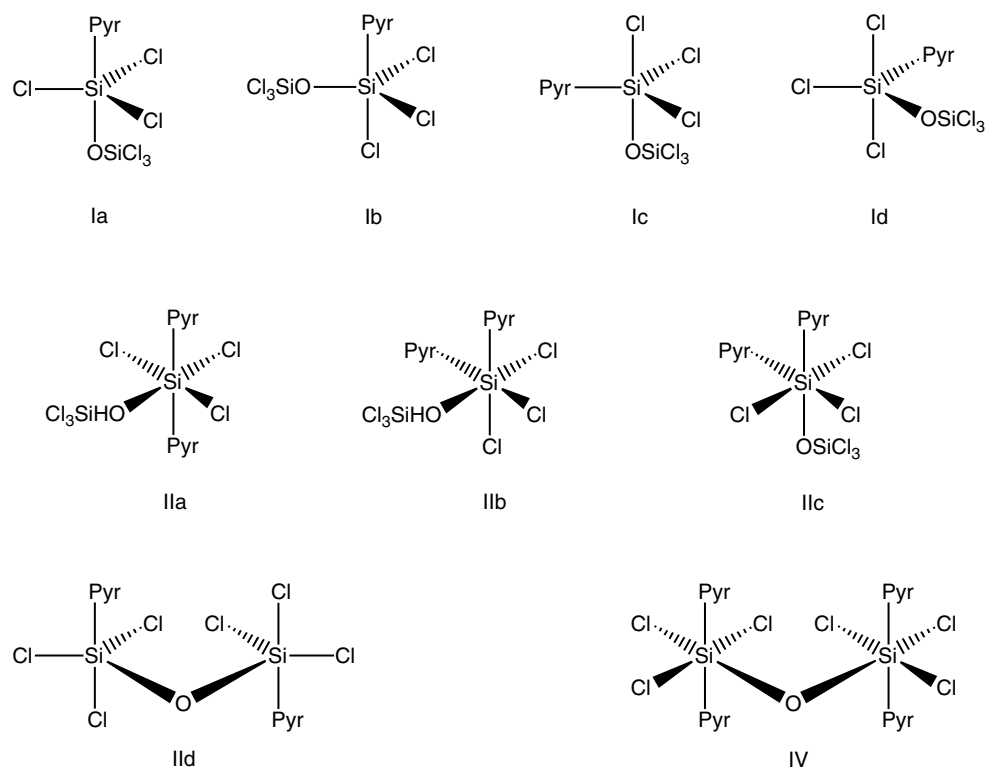


Figure 3. Possible coordination modes of the monodentate ligand pyridine to interact with the two silicon atoms in hexachlorodisiloxane.

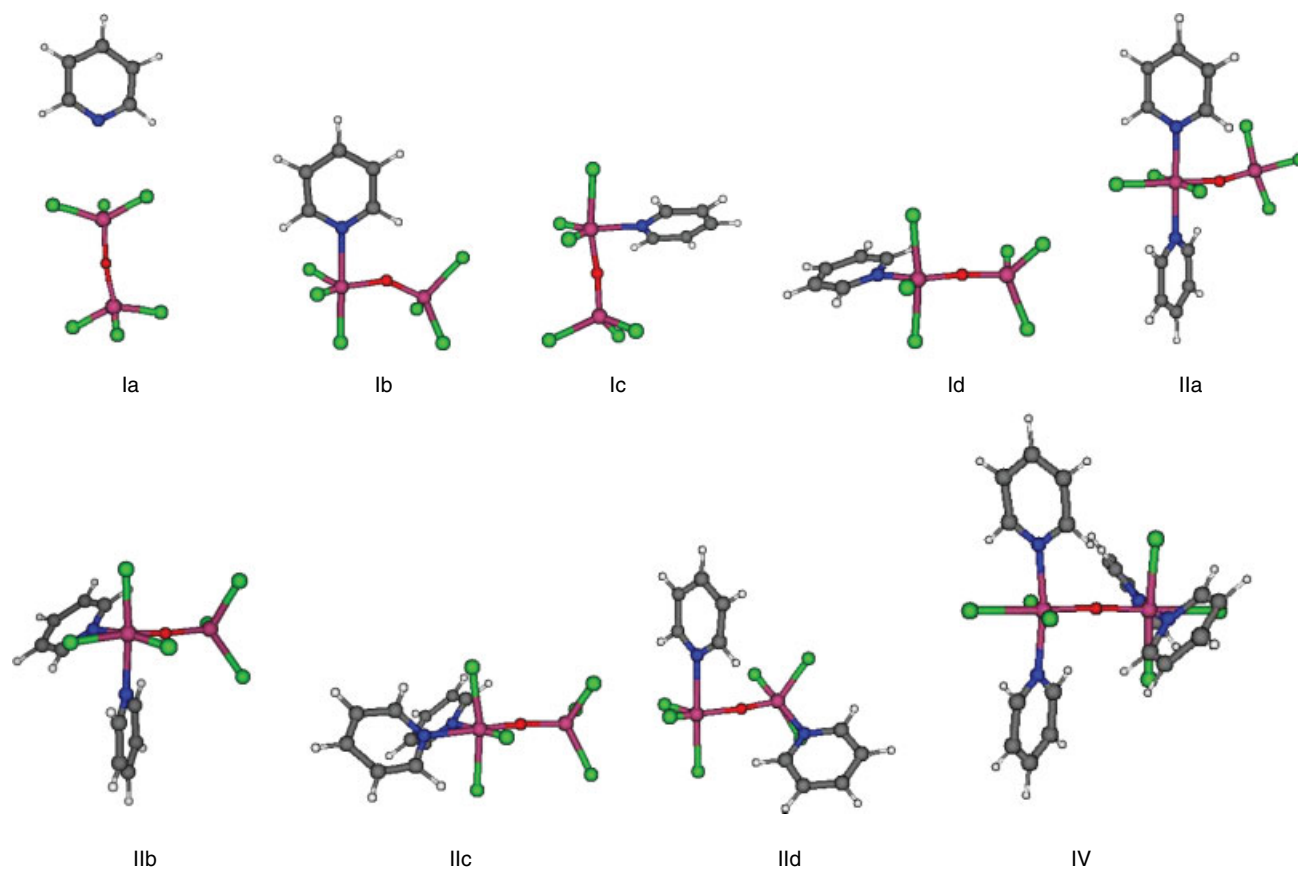


Figure 4. Calculated structures of pyridine-hexachlorodisiloxane adducts shown in Fig. 3.

Table 2. Selected geometrical parameters of complexes shown in Fig. 3

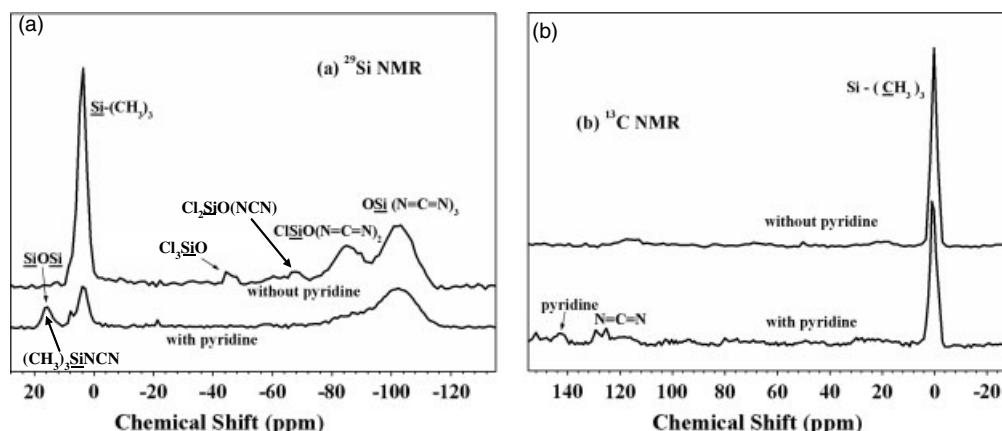
Complex	ΔE (kcal mol ⁻¹) ^a	d(Si-N) (Å)	d(Si-O) (Å)	d(Si-O) ^b (Å)	α (N-Si-N) (deg)
Si ₂ OCl ₆	-	-	-	1.633	-
Ia	-0.10	3.661	1.641	1.626	-
Ib	+4.23	2.248	1.673	1.638	-
Ic	+12.33	1.970	1.739	1.608	-
Id	+12.52	1.960	1.664	1.617	-
IIa	-0.56	2.038	1.745	1.596	179.4
IIb	+4.68	2.134	1.746	1.607	83.9
IIc	+4.89	2.126	1.718	1.609	86.6
IId	+11.29	2.242	1.659	-	-
IV	+14.20	2.049	1.695	-	172.5

^a Relative energies (with respect to reactants).^b Noncoordinated silicon atom.

bonded to three carbodiimide groups and one oxygen atom. This is deduced from the chemical shifts of Si(NCN)₄ (-104 ppm) and SiO₄ units (-110 ppm).^[43,45,46] The signals centered at ca. -85, -68 and -45 ppm indicate the presence of silicon atoms in ClSiO(NCN)₂, Cl₂SiO(NCN) and Cl₃SiO moieties, respectively, in the gel structure.^[45] An additional signal at 3.0 ppm results from trimethylsilyl substituents, i.e. NCN-Si(CH₃)₃ end groups.^[47]

In contrast, for the xerogels obtained *with pyridine* as a catalyst, the signals related to ClSiO(NCN)₂, Cl₂SiO(NCN) and Cl₃SiO groups are much less pronounced, implying an obviously higher crosslinking degree. The strongest signal at ca. -103 ppm is assigned to OSi(N=C=N)₃ units and the peaks around 18 ppm to NCN-Si(CH₃)₃ units.^[48] The latter assignment appears a little inconsistent with the above-mentioned signal at 3 ppm (for specimens obtained without pyridine). However, the said chemical shift range is characteristic for trimethylsilyl groups as reported in literature.^[47,48]

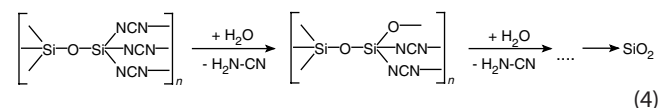
The ¹³C NMR chemical shifts for the NCN groups were detected between 120 and 125 ppm (Fig. 5b).^[8,9,13,15] Without pyridine, a more complex structure is formed, as can be seen from the ²⁹Si CP/MAS NMR, with differently bonded NCN units. This is most likely the reason that the generally weak ¹³C signal for the carbodiimide group is not visible in Fig. 5b (top).

**Figure 5.** (a) ²⁹Si CP/MAS NMR spectrum of Si/C/O/N xerogels at 75 °C aging for 30 days; (b) ¹³C CP/MAS NMR spectrum of Si/C/O/N xerogels at 75 °C aging for 30 days.

The ¹³C NMR peak at around 0.6 ppm results from the residual -Si(CH₃)₃ end groups. Additional signals attributed to pyridine were observed in the samples with catalyst at about 145 ppm.^[13,15]

The FT-IR and Raman spectra of the as-synthesized Si/C/O/N xerogels shown in Fig. 6a and 6b clearly indicate the presence of N=C=N units with the characteristic valence vibrations at 2168 and 1533 cm⁻¹, as well as the corresponding deformation vibration at 800 cm⁻¹. An Si-O-Si absorption band appears at 1100 cm⁻¹.^[49,50] The characteristic valence signal for cyanamide N-C≡N groups at 2264 cm⁻¹. The signal at 570 cm⁻¹ is caused by deformation vibrations of Si-NCN moieties and/or valence vibrations of the Si-Cl groups. A weak signal at 1270 cm⁻¹ is attributed to Si-CH₃ units.^[51]

Like other silylcarbodiimides,^[9,13] Si/C/O/N xerogels are also sensitive to moisture. After 2 h in air, the xerogel hydrolyzes to form Si-O-Si/Si-OH groups and cyanamide (H₂N-CN) or its oligomers, e.g. dicyanamide or melamine as depicted in eqn (4) and Fig. 6(c).^[15,52] The IR signals at 3250 cm⁻¹ appearing in the spectrum in Fig. 6(c) indicate absorptions owing to Si-OH and N-H groups. The expected absorption owing to valence vibration for the cyano moieties at 2264 cm⁻¹ is also present. The additional signals around 1700 cm⁻¹ are caused by N-H deformation vibrations and carbonyl valence vibrations of further hydrolysis products of the cyanamide such as urea.



However, it is at present not clear, how the hydrolytic sensitivity of Si-NCN units is influenced by the number of oxygen atoms bonded to the same silicon atom. This is a matter for further investigation. After thermal treatment at 1000 °C Si/C/O/N ceramics are obtained, which are stable against oxidation and hydrolysis in air (see below).

Morphology and Thermal Behavior of Si/C/O/N xerogels

After different aging times, the gels were dried at 160 °C in vacuum. Analysis of nitrogen adsorption data according to the Brunauer-Emmett-Teller model, shows that the xerogels aged at 75 °C for 30 days with pyridine as catalyst have a surface area of 46 m² g⁻¹. This is a rather low value compared with

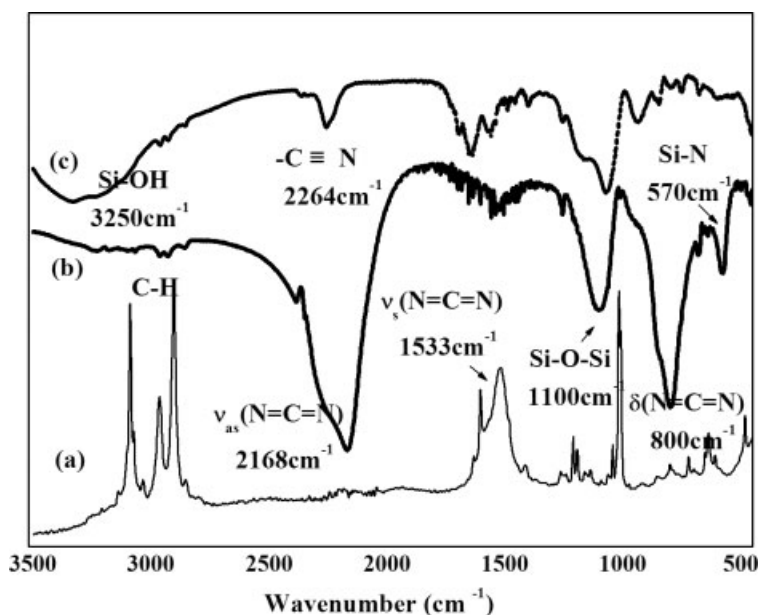


Figure 6. Spectra of a Si/C/O/N xerogel synthesized at 75 °C, aging for 30 days: (a) Raman; (b) FTIR of a xerogel as synthesized; and (c) FT-IR for the same xerogel hydrolyzed in air for 2 h.

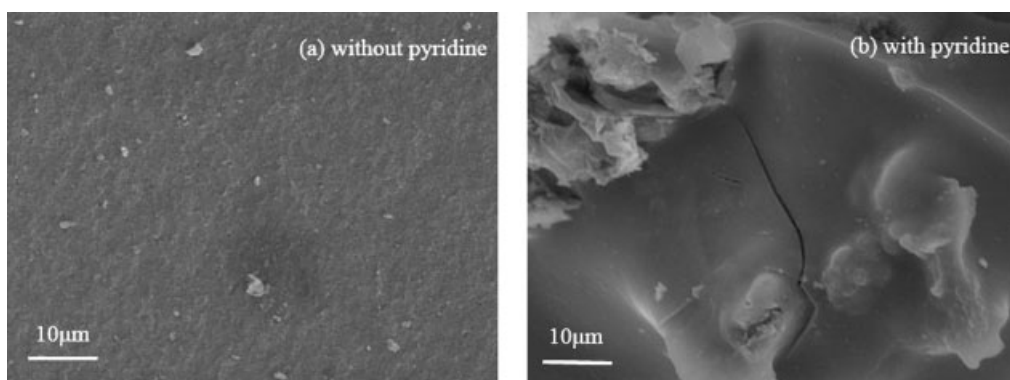


Figure 7. SEM micrographs of Si/C/O/N xerogels showing microstructure typically observed for samples prepared with and without pyridine as a catalyst.

typical data for oxide xerogels, which frequently show specific surface areas in the range of up to 1000 m² g⁻¹ and above.^[1–3] However, carbodiimide-based xerogels have been reported to show comparatively low surface area values.^[11] This may be related to the hydrolytic sensitivity of these materials, which might lead to pore closure resulting from surface reactions (partial hydrolysis and condensation at the surface).

Morphologies of the obtained xerogels were investigated by means of SEM and HR-TEM. SEM micrographs (Fig. 7) indicate the formation of xerogels without any macro-porosity in both samples with pyridine and without pyridine.

Figure 7(a) shows a smooth surface of the xerogel, indicating a homogenous gel process without pyridine. In contrast, with pyridine as catalyst (Fig. 7b), the gel appears to be more heterogeneous. The above-discussed formation of adducts of the type [RSiCl₃ · 2Py] may be responsible for this observation. Nevertheless, the reaction with pyridine proceeds more completely than without it in the same period of time, which agrees with the solid-state NMR results (see above).

The thermal behavior of the obtained Si/C/O/N xerogels was investigated by thermal gravimetry (TGA) under argon

(Fig. 8). It should be pointed out that these studies are not directly comparable with the bulk ceramisation performed under ammonia. It is known that pyrolysis of Si/C/N and related Si/E/C/N precursor polymers under NH₃ induces substitution and transamination reactions as well as the formation of volatile C_xH_y species, resulting in a decreased carbon and an increased nitrogen content of the ceramics.^[53,54] The results of the TGA measurements show that the ceramic yield depends on the synthesis temperature and aging time of the gels but is not influenced by the content of catalyst.

Figure 8(a) shows that the ceramic yields of the xerogels with or without pyridine as catalyst are the same, even though the decomposition paths are different. With pyridine, the degree of cross-linking should be higher. However, the removal of residual pyridine in the xerogel can lead to an increased weight loss. Under higher aging temperature and after longer aging time, the ceramic yield increases from about 43 to 51%, as can be seen in Fig. 8(b and c), which indicates that the cross-linking reactions to form gels are more complete in these xerogels. It should be pointed out that the TGA investigations performed under argon atmosphere are not directly comparable with the bulk pyrolyses discussed in

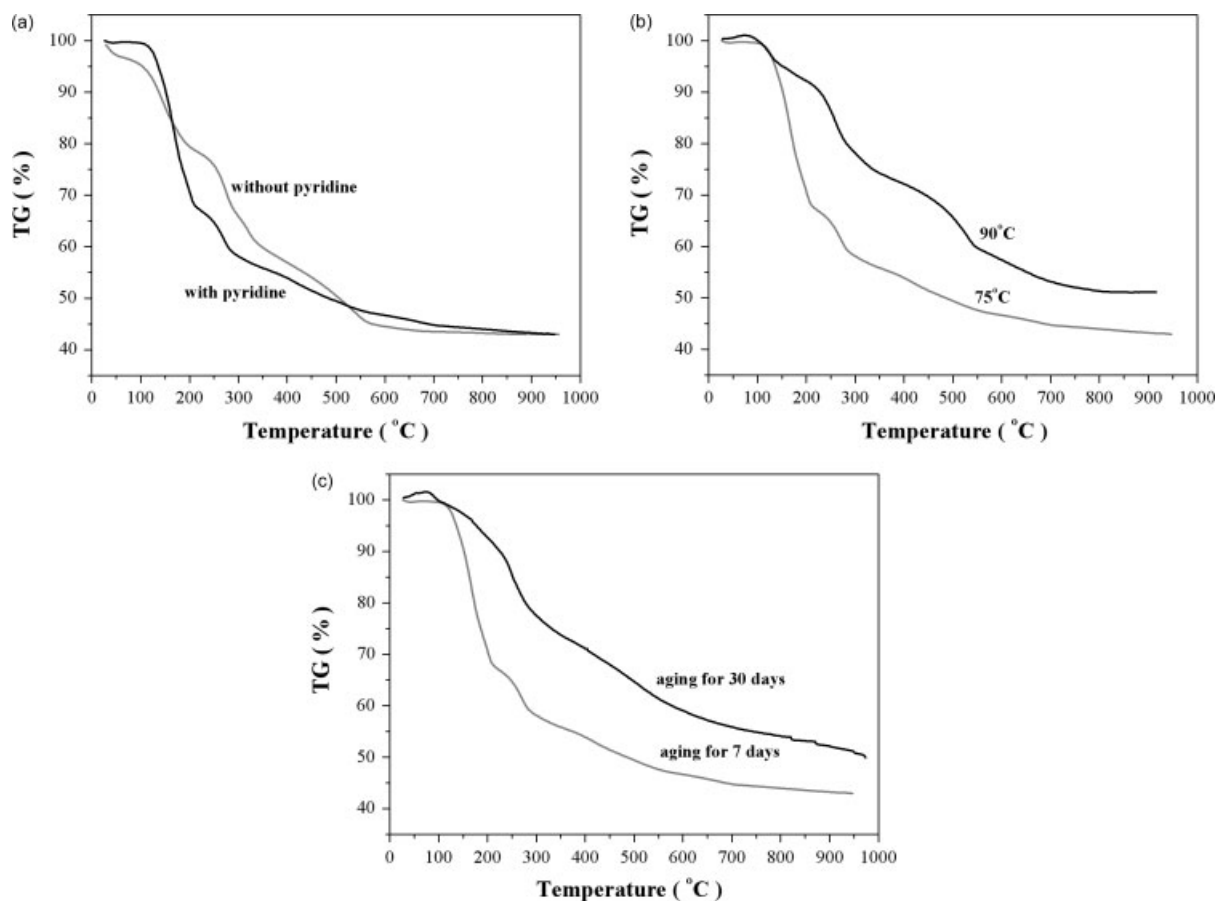


Figure 8. Thermogravimetry curves of Si/C/O/N xerogels: (a) aging for 7 days at 75 °C with or without pyridine; (b) with pyridine aging for 7 days at 75 and 90 °C; and (c) with pyridine at 75 °C aging for 7 and 30 days.

the following chapter. Argon acts as an inert gas which does not undergo any chemical reactions with the xerogels, ceramics or gaseous side products,

Chemical Structure of Silylcarbodiimide-derived Si/C/O/N ceramics

Bulk pyrolyses of the xerogels were performed under ammonia atmosphere. This induces transamination and substitution reactions reducing the number of -NCNSiMe_3 end groups and Si-Cl units. At higher temperatures the carbon content is decreased while nitrogen is incorporated.^[53] FT-IR spectra of products obtained from gels synthesized with and without pyridine and pyrolyzed at 1000 °C show absorption bands $\nu(\text{NCN})$ at $\sim 2200 \text{ cm}^{-1}$, which indicates that carbodiimide units are still present (Fig. 9a). This is supported by solid-state ^{13}C NMR spectra showing a broad resonance signal centered at $\sim 100 \text{ ppm}$, which is characteristic for N=C=N units (Fig. 9b). However, the broadness of this ^{13}C NMR signal and the weakness of the FT-IR signal seem to indicate that a major part of the carbodiimide units is decomposed. A rearrangement to the isomeric cyanamide group N-CN is also possible. Such cyanamide carbons typically appear at 115 ppm in the ^{13}C NMR spectra.^[13] Nevertheless, a surprisingly high thermal stability of the NCN moiety up to 1000 °C was also found for other silylcarbodiimides.^[11] However, it should be pointed out that most authors examining the pyrolysis of polysilylcarbodiimides used argon and nitrogen atmospheres.

The ^{29}Si NMR resonance centered at -50 ppm for the same sample (Fig. 9c) is in the chemical shift range reported for amorphous silicon nitride, $\text{Si}_2\text{N}_2\text{O}$ as well as $\text{Si}_2\text{N}_2(\text{NCN})$.^[11] No further details can be concluded owing to the broadness and featureless nature of the resonance (see below). This indicates that rather random Si/C/O/N networks with a low degree of order and crystallinity are characteristic for the samples synthesized at 1000 °C, as expected. The predominantly amorphous nature with only weak indications for partial nanocrystallinity of these products was confirmed by powder XRD measurements (Fig. 10) as well as several HR-TEM studies (see below).

The position of the ^{29}Si NMR signal together with the strong absorption band in the FTIR spectrum (Fig. 9a) around 950 cm^{-1} indicate that the network is primarily composed of Si-N and Si-O bonds. Si-C units are not present after pyrolysis at 1000 °C (an FT-IR absorption at $700\text{--}800 \text{ cm}^{-1}$ would be expected). The carbon is obviously primarily bonded to nitrogen in the form of NCN units (in the carbodiimide and/or cyanamide form). No free carbon was detectable by the applied methods (no G or D band in the FT-IR spectrum; no graphitic structures in HR-TEM, see below).

Further information on the chemical structure of the amorphous ceramics obtained upon pyrolysis at 1000 °C may be gained from detailed analysis of the elemental composition and element distribution. Several samples were therefore investigated by combustion analyses, EDX and EELS. Chlorine was not detected in the samples. Depending on the various processing parameters which include synthesis of the xerogel precursors (catalyst,

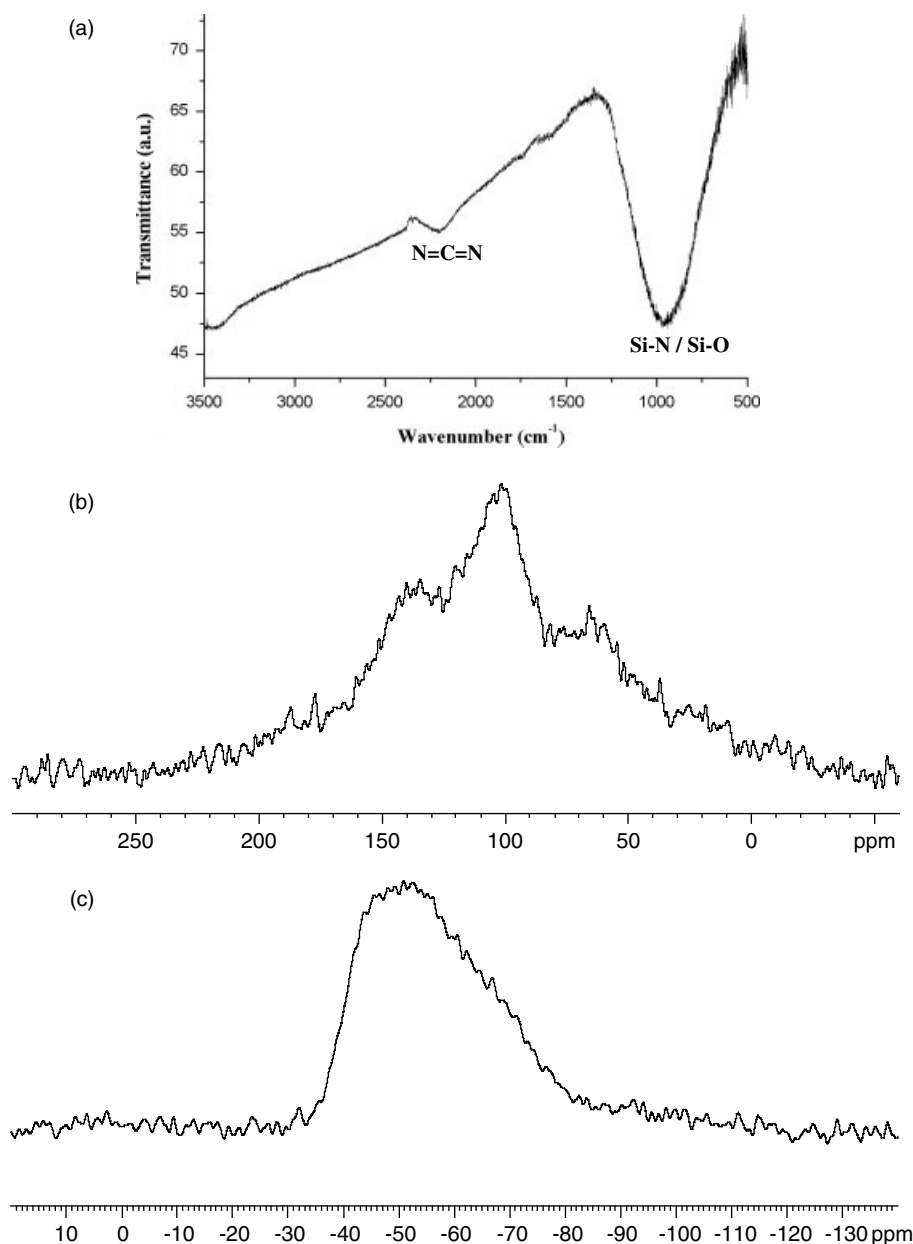


Figure 9. FTIR (a), ¹³C (b) and ²⁹Si (c) solid state NMR spectra of the Si/C/O/N xerogel pyrolyzed under NH₃ at 1000 °C.

temperature, aging time, solvent) and pyrolysis conditions (NH₃ atmospheres, powder or bulk sample, heating rate, annealing temperature and holding time) the overall composition varied significantly in the range of Si, 36–49; C, 2–24; N, 20–28; O, 10–19 (weight-%). This has to be compared with the ideal composition of a [SiOSi(NCN)₃]_n with completely intact carbodiimide groups and Si₂N₂O which may be obtained upon full decomposition of the carbodiimide units and complete removal of the carbon, i.e. Si, 29.1; C, 18.8; N, 43.8; O, 8.3 and Si, 56.0; C, 0.0; N, 28.0; O, 16.0, respectively. In general, we found a decreasing carbon content with increased pyrolysis temperatures especially in ammonia atmospheres. This is expected owing to the reactions of NH₃ to form volatile carbon compounds such as cyanamide H₂N–CN and its dimer cyanoguanidine and trimer melamine, HCN or methane, which all lead to a decreased carbon content of the solid residue.^[53,54] Selected ceramic products were thoroughly

investigated with EELS. The EEL-spectra of samples pyrolyzed under NH₃ at 1000 °C show very similar features to Si₂N₂O, which contains the analogous OSiN₃-units (Fig. 11).

Morphology of Silylcarbodiimide-derived Si/C/O/N ceramics

HR-TEM studies on xerogel samples synthesized at 75 °C and pyrolyzed at 1000 °C under ammonia atmosphere clearly show that mesoporous Si/C/O/N materials are formed. Typical TEM images are shown in Fig. 12(a, b). An amorphous and very porous microstructure was observed in powdered as well as bulk samples. Nitrogen adsorption measurements did not show any significant porosity, indicating that the pores are closed.

A statistical analysis of the pore sizes (open as well as closed pores observed by TEM) indicates a rather narrow size distribution with an average pore diameter of 16.4 ± 0.4 nm (Fig. 13). This

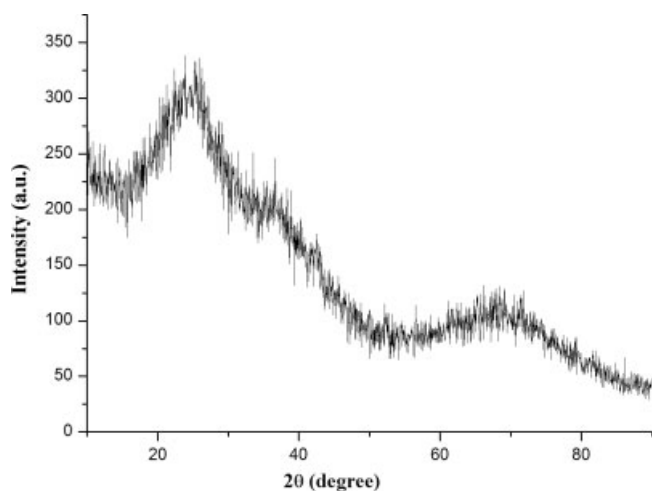


Figure 10. XRD pattern of the sample pyrolyzed in NH_3 at 1000°C , indicating the amorphous nature of the solid.

corresponds well with investigations on the preparation of silylcarbodiimide-derived Si/C/N membranes.^[22]

Preliminary investigation of the pyrolysis behavior above 1000°C indicates that pore sizes significantly decrease to values around 10 nm. Graphitic carbon is not detectable, but nano-sized carbon domains segregate around 1400°C . Silicon nitride starts to crystallize in the same temperature range. A detailed investigation of the crystallization behavior of the amorphous Si/C/O/N ceramics and the dependence of the Si/C/O/N network structure after annealing at various temperatures on the structure and chemical

composition of the starting polymer is the major point of interest for our future work. While for Si/C/O materials a purely statistical distribution among possible $\text{SiC}_{4-x}\text{O}_x$ sites has been reported,^[55] a strong influence of the precursor structure on the ceramic structure has been found for Si/C/N materials, especially when silazanes are compared with silylcarbodiimides.^[56]

Conclusions

The following conclusions can be drawn from the reported investigations:

- (1) The sol-gel preparation of hybrid polysiloxane/poly-silylcarbodiimide gels, i.e. the controlled introduction of oxygen into Si/C/N xerogels and ceramics, is reported for the first time. The pyridine-catalyzed gel formation and cross-linking between hexachlorodisiloxane ($\text{Cl}_3\text{Si-O-SiCl}_3$) and *bis*(trimethylsilyl)carbodiimide can be performed at temperatures between 40 and 90°C .
- (2) Amorphous, hydrolytically sensitive xerogels are obtained, which consist of a random network of Si-O-Si and Si-NCN-Si units. The same structural feature is present in the macrocyclic molecule $[\text{SiPh}_2\text{-O-SiPh}_2(\text{NCN})_2]$. NMR data and a single crystal structure of this compound provide detailed information as a model for the chemical structure of the Si/C/O/N gels.
- (3) The gelation time is decreased with increasing temperature and increasing the amount of pyridine. In the latter case, precipitates of pyridine-chlorosilane adducts were observed, consisting of the hexacoordinated chlorosilane

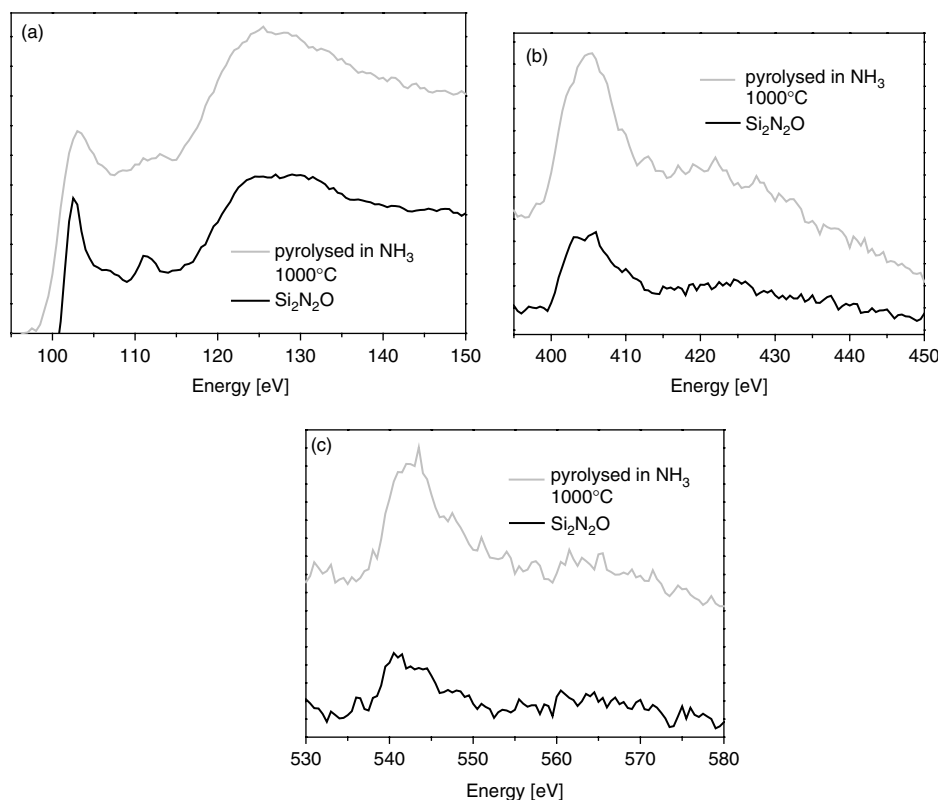


Figure 11. EEL-spectra of Si/C/O/N ceramics obtained by pyrolysis of the xerogel in NH_3 at 1000°C in comparison with the spectra of silicon oxynitride $\text{Si}_2\text{N}_2\text{O}$. Si-L_{2,3} edge (a); N-K edge (b); and O-K edge (c).

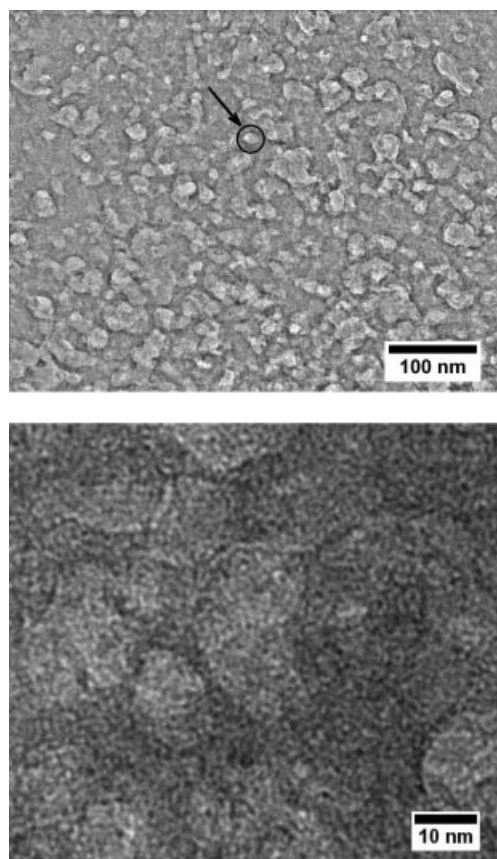


Figure 12. TEM (a) and HR-TEM (b) micrographs of a typical Si/C/O/N xerogel obtained by a pyridine-catalyzed reaction of hexachlorodisiloxane with BTSC after aging and drying followed by pyrolysis under dry ammonia at 1000 °C. The amorphous material is characterized by homogeneously distributed, irregular mesopores as marked by the arrow in (a).

adduct $\text{Cl}_3\text{Si}-\text{O}-\text{SiCl}_3(\text{Py})_2$, which was structurally analyzed by single crystal X-ray diffraction. Interestingly, only one of the two Si atoms is activated by coordination to pyridine. The latter observation was also supported by theoretical investigations.

- (4) There is neither a negative effect of the $\text{Cl}_3\text{Si}-\text{O}-\text{SiCl}_3(\text{Py})_2$ precipitates on the gelation process, nor a positive effect of the pyridine-catalyzed cross-linking on the ceramic yield after pyrolysis of the xerogels. Instead, the reaction temperature and aging time are crucial for complete cross-linking. However, there are significant differences in the structure and morphology of the xerogels obtained with and without pyridine.
- (5) Pyrolysis at temperatures up to 1000 °C gives amorphous Si/C/O/N ceramics accompanied by a mass loss of about 50%. The products still contain residual carbodiimide units.
- (6) Depending on the pyrolysis atmospheres and other processing parameters (such as synthesis and aging conditions of the xerogels) chemical compositions and structures intermediate between the ideal polymeric $[\text{SiOSi}(\text{NCN})_3]_n$ and the silicon oxynitride $\text{Si}_2\text{N}_2\text{O}$ are formed. The products obtained at 1000 °C are mesoporous, the pore size decreases upon annealing at higher temperatures.

Further work will focus on different methods for synthesizing the Si/C/O/N materials and annealing at different temperatures

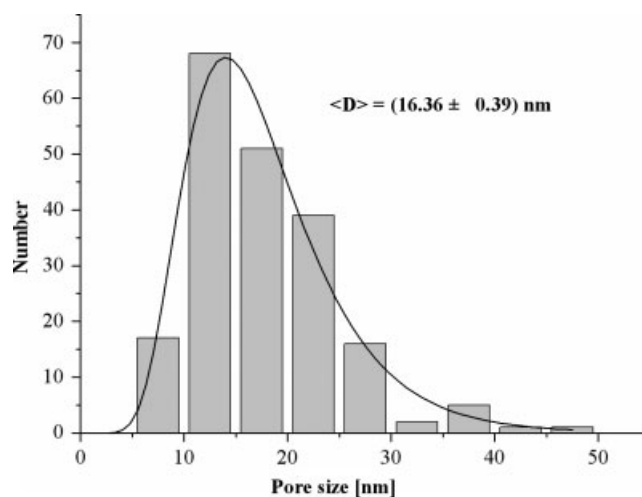


Figure 13. Pore size distribution derived by measuring the diameters of 200 of the pores shown in the HR-TEM micrographs in Fig. 8. An average pore diameter of 16.4 ± 0.4 nm was determined.

above 1000 °C and in different atmospheres to form (partially) crystalline ceramics.

Acknowledgment

This work was supported by the Deutsche Forschungsgemeinschaft, DFG (Project KR 1739/18-1 and WO 482/19-1), the CSC (China Scholarship Council) project and a cooperation between TU Bergakademie Freiberg and Tianjin University, China. The authors thank the colleagues of the Departments of Chemistry and of Material Science at TU Bergakademie Freiberg, Germany, for the analysis work (NMR, XRD, FTIR, RAMAN, SEM, TEM, elemental analyses, and nitrogen adsorption method).

Supporting information

Supporting information may be found in the online version of this article.

References

- [1] C. J. Brinker, G. W. Scherer, *Sol-Gel Science*, **1990**, Academic Press: San Diego, CA.
- [2] L. L. Hench, J. K. West, *Chem. Rev.* **1990**, *90*, 33.
- [3] R. Uhlmann, D. R.; Ulrich, *Adv. Mater. Opt. Electron.* **1993**, *2*, 151.
- [4] See e.g. A. González-Campo, B. Boury, F. Teixidor, R. Núñez, *Chem. Mater.* **2006**, *18*, 4344.
- [5] See e.g. R. Harshe, C. Balan, R. Riedel, *J. Eur. Ceram. Soc.* **2004**, *24*, 3471.
- [6] A. Kienzle, J. Bill, F. Aldinger, R. Riedel, *Nanostruct. Mater.* **1995**, *6*, 349.
- [7] R. Riedel, A. Greiner, G. Miehe, W. Dressler, H. Fuess, J. Bill, F. Aldinger, *Angew. Chem. Int. Ed.* **1997**, *36*, 603.
- [8] O. Gabriel, R. Riedel, *Angew. Chem., Int. Ed.* **1997**, *36*, 384.
- [9] O. Gabriel, R. Riedel, S. Storck, W. F. Maier, *Appl. Organomet. Chem.* **1997**, *11*, 833.
- [10] O. Gabriel, R. Riedel, W. Dressler, S. Reichert, *Chem. Mater.* **1999**, *11*, 412.
- [11] R. Riedel, E. Kroke, A. Greiner, A. O. Gabriel, L. Ruwisch, J. Nicolich, P. Kroll, *Chem. Mater.* **1998**, *10*, 2964.
- [12] D. S. Kim, E. Kroke, R. Riedel, A. O. Gabriel, S. C. Shim, *J. Appl. Organomet. Chem.* **1999**, *13*, 495.
- [13] K. Lippe, J. Wagler, E. Kroke, S. Herkenhoff, V. Ischenko, J. Woltersdorf, *Chem. Mater.* **2009**, *21*, 3941.

- [14] G. Mera, A. Tamayo, H. Nguyen, S. Sen, R. Riedel, *J. Am. Ceram. Soc.* **2010**, *93*, 1169.
- [15] S. N. Borchert, E. Kroke, R. Riedel, B. Boury, R. J. P. Corriu, *J. Organomet. Chem.* **2003**, *686*, 127.
- [16] C. Balan, K. W. Völger, E. Kroke, R. Riedel, *Macromolecules* **2000**, *33*, 3404.
- [17] E. Kroke, *Organosilicon Chemistry VI – From Molecules to Materials*, Vol. 1, Wiley-VCH: Weinheim, **2005**, 160.
- [18] E. Kroke, A. O. Gabriel, R. Riedel, *Flüssigphasendarstellung von SiC, Werkstoffwoche '98*, Band VII, Wiley-VCH: Weinheim **1999**, 297.
- [19] E. Kroke, K. W. Völger, A. Klönczynski, R. Riedel, *Angew. Chem. Int. Ed.* **2001**, *40*, 1698.
- [20] W. Völger, E. Kroke, R. Riedel, C. Gervais, F. Babonneau, T. Saitou, Y. Iwamoto, *Chem. Mater.* **2003**, *15*, 755.
- [21] Y.-L. Li, E. Kroke, A. Klönczynski, R. Riedel, *Adv. Mater.* **2000**, *12*, 956.
- [22] K. W. Voelger, R. Hauser, E. Kroke, R. Riedel, Y. H. Ikuhara, Y. Iwamoto, *J. Ceram. Soc. Japan* **2006**, *114*, 567.
- [23] M. Weinmann, R. Haug, J. Bill, M. De Guire, F. Aldinger, *Appl. Organomet. Chem.* **1998**, *12*, 725.
- [24] M. Weinmann, M. Hoerz, A. Mueller, F. Aldinger, in *Organosilicon Chemistry VI: From Molecules to Materials*, Vol. 2 (Eds.: N. Auner, J. Weis), Wiley-VCH: Weinheim **2005**, 987.
- [25] A. Gonzalez-Campo, R. Nunez, C. Vinas, B. Boury, *New J. Chem.* **2006**, *30*, 546.
- [26] F. Berger, M. Weinmann, F. Aldinger, K. Mueller, *Chem. Mater.* **2004**, *16*, 919.
- [27] C. Ritter, A. V. G. Chizmeshya, T. L. Gray, J. Kouvetakis, *Appl. Organomet. Chem.* **2007**, *21*, 595.
- [28] A. Trifonov, D. M. Lyubov, E. A. Fedorova, G. G. Skvortsov, G. K. Fukin, Yu. A. Kurskii, M. N. Bochkarev, *Russ. Chem. Bull.* **2006**, *55*, 435.
- [29] R. M. Morcos, G. Mera, A. Navrotsky, T. Varga, R. Riedel, F. Poli, K. Muller, *J. Am. Ceram. Soc.* **2008**, *91*, 3349.
- [30] S. Shoji, JP 2010174133 A 20100812.
- [31] F. Shriver, *The Manipulation of Air-sensitive Compounds*, McGraw-Hill: New York, **1969**, 299.
- [32] A. Vostokov, Y. I. Dergunov, A. S. Gordetsov, *Zh. Obshch. Khim.* **1977**, *47*, 1769.
- [33] M. W. Schmidt, K. K. Baldrige, J. A. Boatz, S. T. Elbert, M. S. Gordon, J. J. Jensen, S. Koseki, N. Matsunaga, K. A. Nguyen, S. Su, T. L. Windus, M. Dupuis, J. A. Montgomery, *J. Comput. Chem.* **1993**, *14*, 1347.
- [34] D. Glendening, J. K. Badenhop, A. E. Reed, J. E. Carpenter, J. A. Bohmann, C. M. Morales, F. Weinhold, *NBO 5.0*, Theoretical Chemical Institute, University of Wisconsin: Madison, WI, **2001**.
- [35] W. J. Hehre, R. Ditchfield, L. Radom, J. A. Pople, *J. Am. Chem. Soc.* **1970**, *92*, 4796.
- [36] O. Bechstein, B. Ziemer, D. Haas, S. I. Troyanov, V. B. Rybakov, G. N. Maso, *Z. Anorg. Allg. Chem.* **1990**, *582*, 211.
- [37] G. W. Fester, J. Wagler, E. Brendler, E. Kroke, *Eur. J. Inorg. Chem.* **2008**, 5020.
- [38] G. W. Fester, J. Wagler, E. Brendler, U. Böhme, G. Roewer, E. Kroke, *Chem. Eur. J.* **2008**, *14*, 3164.
- [39] G. W. Fester, J. Wagler, E. Brendler, U. Böhme, D. Gerlach, E. Kroke, *J. Am. Chem. Soc.* **2009**, *131*, 6855.
- [40] G. Fester, J. Eckstein, J. Wagler, E. Brendler, E. Kroke, *Inorg. Chem.* **2010**, *49*, 2667.
- [41] H. C. Marsmann, E. Meyer, M. Vongehr, E. F. Weber, *Makromol. Chem.* **1983**, *184*, 1817.
- [42] W. Airey, C. Glidewell, A. G. Robiette, G. M. Sheldrick, *J. Mol. Struct.* **1971**, *8*, 413.
- [43] O. Gabriel, Darstellung und Keramisierung sauerstoffreier Polysilylcarbodiimid-Gele PhD Thesis, **1998**, Darmstadt University of Technology.
- [44] N. Hering, K. Schreiber, R. Riedel, O. Lichtenberger, J. Woltersdorf, *Appl. Organomet. Chem.* **2001**, *15*, 879.
- [45] A. Greiner, Keramiken aus Silylcarbodiimiden, PhD Thesis **1997**, Darmstadt University of Technology.
- [46] H. Marsmann, *NMR-basic Principles and Progress*, Springer: Berlin, **1981**.
- [47] H. C. Marsmann, *Chem. Zeit.* **1972**, *96*, 288.
- [48] Y. Ivanova, T. Gerganova, H. M. H. V. Fernandes, I. M. M. Salvado, E. Kashchieva, *J. Uni. Chem. Tech. Matal.* **2006**, *41*, 311.
- [49] K. Nakamoto, *Infrared and Raman Spectra of Inorganic and Coordination Compounds*, 3rd edn, John Wiley and Sons: New York **1978**, 448.
- [50] J. Weidlein, U. Mueller, K. Dehnicke, *Vibrational Frequencies, Vol. 1: Main Group Elements*, Thieme: Stuttgart, **1981**, 339.
- [51] Y. P. Zhou, D. Probst, A. Thissen, E. Kroke, R. Riedel, *et al.*, *J. Eur. Ceram. Soc.* **2006**, *26*, 1325.
- [52] P. Barrett, L. Joyner, P. P. Halenda, *J. Am. Chem. Soc.* **1951**, *73*, 373.
- [53] E. Kroke, Y.-L. Li, C. Konetschny, E. Lecomte, C. Fasel, R. Riedel, *Mater. Sci. Eng. R* **2000**, *26*, 97.
- [54] N. S. Choong Kwet Yive, R. J. P. Corriu, D. Leclercq, P. H. Mutin, A. Vioux, *Chem. Mater.* **1992**, *4*, 1263.
- [55] P. H. Mutin, *J. Am. Ceram. Soc.* **2002**, *85*, 1185.
- [56] Y. Iwamoto, W. Völger, E. Kroke, R. Riedel, T. Saitou, K. Matsunaga, *J. Am. Ceram. Soc.* **2001**, *84*, 2170.